

## Crystal and Quasicrystal Structures in Al-Mn-Si Alloys

Veit Elser and Christopher L. Henley<sup>(a)</sup>

AT&T Bell Laboratories, Murray Hill, New Jersey 07974

(Received 12 July 1985)

We show that the  $\alpha$ -(AlMnSi) crystal structure is closely (and systematically) related to that of the icosahedral Al-Mn-Si alloys. Using a modification of the "projection" method of generating icosahedral structures from six-dimensional lattices, we find a simple description of the  $\alpha$ -(AlMnSi) structure. This structure, and (we conjecture) the icosahedral one, can also be described as a packing of 54-atom icosahedral clusters.

PACS numbers: 61.55.Hg, 61.50.Em

The discovery of a rapidly cooled alloy  $i$ -(AlMn) having an icosahedral point diffraction pattern<sup>1</sup> has posed fascinating crystallographic problems. The supposed incompatibility of icosahedral symmetry and long-range positional order was quickly resolved by the construction of an ordered aperiodic structure ("quasicrystal") with an icosahedral diffraction pattern.<sup>2</sup> Subsequently, phenomenological Landau theories appeared which explored the symmetries and (meta)stability of a substance with icosahedral density waves.<sup>3-8</sup> A complementary approach<sup>3,9-11</sup> has used as a model the three-dimensional Penrose tiling (3DPT), an aperiodic lattice (described below) which has the same diffraction pattern as  $i$ -(AlMn).

Still unknown is the microscopic structure (atomic positions) of  $i$ -(AlMn). Besides being intrinsically interesting in light of the novel symmetry, structural information is essential to studies of electronic structure, the existence of phasons,<sup>3-5</sup> etc. Direct determination of the structure from diffraction is unfeasible with present samples (crystallite diameters  $\leq 2 \mu\text{m}$ ); only a few peaks (in the expected dense pattern) can be resolved in x-ray powder patterns,<sup>12</sup> while electron-diffraction intensities are generally difficult to interpret. Although technical improvements will ultimately be required to refine any proposed structure, we present here a particular analysis of related *crystalline* structures<sup>13-15</sup> on which such a proposal might be based.

Our strategy for connecting the crystal and quasicrystal structures is based on the fact that the 3DPT is the limit of a sequence of *periodic* structures with ever larger unit cells. We start with the convenient (and insightful) construction of the 3DPT as a projection from a six-dimensional hypercubic lattice with the three-dimensional projection hyperplane at an incommensurate orientation.<sup>3,9,10,16</sup> The relation of such a structure to a periodic one is illustrated in Fig. 1, which shows one-dimensional tilings with long (L) and short (S) line segments. In both Figs. 1(a) and 1(b) the tiling elements are generated by the projection of the edges of a two-dimensional lattice into a line AB with slope  $\tau = (1 + \sqrt{5})/2$ . In (a) the selection of

edges for projection is accomplished by a strip also having slope  $m = \tau$ , whereas in (b) the strip is tilted to have slope  $m' = 2/1$ . Construction (a) generates the well-known one-dimensional analog<sup>2</sup> of the Penrose tiling while (b) generates a periodic structure composed of the *same* tiling elements. By choosing  $m'$  to be a continued-fraction approximant to  $\tau$  ( $m' = 2/1, 3/2, 5/3, \dots$ ), one creates structures with larger periods which approximate the aperiodic tiling of (a) better and better. In the same sense that "finite" continued fractions are rational, we use the word "finite" to describe periodic tilings such as in Fig. 1(b).

By a similar modification of the projection construction of the 3DPT, it is possible to generate finite 3DPT's with a cubic (hexagonal, tetragonal, etc.) structure. In the six-dimensional construction the analog of the strip in Fig. 1 is the product of a three-plane and a suitable three-dimensional "cross section."<sup>9,10</sup> The analogs of the L and S segments are prolate and oblate rhombohedra (PR and OR) with edges of length  $a_R$  oriented in the twelve icosahedral (center-to-vertex) directions. If the orientation in six dimensions of the strip's three-plane is given by the three spanning vectors<sup>17</sup>  $(p, p, q, 0, 0, q)$ ,  $(q, -q, 0, p, p, 0)$ , and  $(0, 0, p, q, -q, -p)$ , then the 3DPT results when  $p/q \rightarrow \tau$ . By taking instead the rational approximants  $p/q = 1/0, 1/1, 2/1, \dots$ , one obtains a sequence of

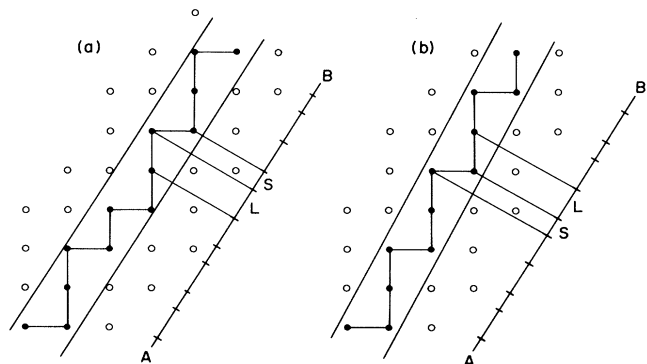


FIG. 1. (a) Incommensurate strip generating quasiperiodic tiling; (b) commensurate strip generating periodic tiling.

(periodic) cubic structures with corresponding lattice constants  $a$ ,  $a\tau$ ,  $a\tau^2$ , . . . [ $a = (2 + 2/\sqrt{5})^{1/2}a_R$ ]. The number ratio  $n_P/n_O$  of PR and OR needed to tile the unit cell in these structures is 4/4, 20/12, 84/52, . . . — a sequence that approaches the value  $\tau$  known for the 3DPT. Kuriyama and Long<sup>18</sup> have recently described a cubic structure based on the 1/0 tiling.

A study of the metallurgical literature has uncovered a number of large-cell Al-transition-metal phases which are candidates for description in terms of finite 3DPT's.<sup>19</sup> Of the relatively few whose structures are known we have been able to identify the phases  $\alpha$ -(AlMnSi)<sup>14</sup> and  $\alpha$ -(AlFeSi)<sup>15</sup> as instances where this description is not only illuminating but also reasonably accurate. We show below that the 1/1 cubic tiling describes the structure of  $\alpha$ -(AlMnSi).

One way to appreciate the fact that  $\alpha$ -(AlMnSi) is quite a good "approximation" to  $i$ -(AlMn) (in the sense of the above discussion) is to compare electron-diffraction patterns. Choosing the Ewald plane normal to (100), we see that the strong peaks in the  $\alpha$ -(AlMnSi) pattern<sup>13</sup> [Fig. 2(a)] agree extremely well with the positions of peaks in the twofold pattern of  $i$ -(AlMn).<sup>9</sup> The calculated intensities shown in Fig. 2(b) are based on a 3DPT model with pointlike atoms at the rhombohedron vertices<sup>9</sup> and agree well with observed intensities.<sup>11,12</sup> (In the structure we are about to describe the strongly scattering Mn atoms do sit on vertices.) The intensities in Fig. 2(a) have been calculated by use of appropriate atomic form factors for all the atoms in the unit cell.<sup>20</sup> The geometric relationship  $|G_B|/|G_A| = \tau$  for peaks  $A'$  and  $B'$  of the icosahedral phase is approximated in the  $\alpha$  phase by  $|G_B|/|G_A| = \frac{5}{3}$ . Similarly, lines from the origin to peaks  $C'$  and  $C$  have respectively slopes  $\tau$  and  $\frac{5}{3}$  in the two phases. Also noteworthy is the agreement in *scale*

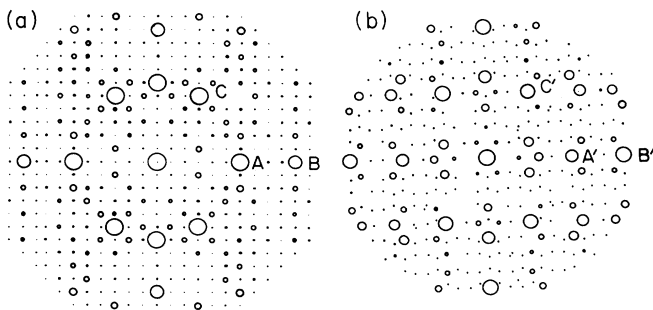


FIG. 2. Calculated electron-diffraction patterns of two 3D structures. The intensity of each spot is represented by its area. (a) The [100] pattern of the cubic  $\alpha$ -(AlMnSi) structure using the atomic coordinates of Ref. 14. (b) The twofold pattern of the 3D Penrose tiling of icosahedral rhombohedra with point scatterers at the vertices.

of the two patterns. In terms of the real-space structure, Fig. 2(b) implies a rhombohedron edge length  $a_R = 4.60$  Å.<sup>11</sup> On the other hand, the lattice constant of  $\alpha$ -(AlMnSi) is  $a\tau = 12.68$  Å which implies  $a_R = 4.61$  Å in the 1/1 tiling.

Another observation suggesting the relevance of  $\alpha$ -(AlMnSi) is that its composition<sup>14</sup> ( $\text{Al}_{72.5}\text{Mn}_{17.4}\text{Si}_{10.1}$ ) is close to the best composition ( $\text{Al}_{74}\text{Mn}_{20}\text{Si}_6$ ) of melt-quenched  $i$ -(AlMnSi).<sup>21</sup> The  $i$ -(AlMnSi) material is superior in quality to  $i$ -(AlMn) in the following three ways<sup>21</sup>: (1) Bragg spots are significantly sharper and more of the weaker spots are resolved. (2) Grains have smooth morphology and more uniform bright-field contrast. (3) The transformation temperature to an unidentified crystalline phase is  $\sim 200$  K higher than the corresponding temperature for  $i$ -(AlMn). A related phase  $i$ -(AlFeSi) probably also exists which should be compared to  $\alpha$ -(AlFeSi) with composition<sup>15</sup>  $\text{Al}_{70.9}\text{Fe}_{19.0}\text{Si}_{10.1}$ ; we show below that the structure of  $\alpha$ -(AlFeSi) can be described as a slightly imperfect tiling.

To specify atomic positions, we use the concept of "decoration" which is inspired by the analogy between the two rhombohedral "Penrose" cells and the unit cell of an ordinary periodic lattice. In a decoration, cells are assigned to classes according to their (generally different) local environments, and within each class atoms sit at essentially identical sites in the cells. The key to an economical description of our decoration is to group two PR and two OR that pack around a single vertex into an additional packing unit, the rhombic dodecahedron (RD); see Fig. 3(a). This combination is also common in the 3DPT.

In our idealized  $\alpha$ -(AlMnSi) structure there are six classes of sites: a large vacancy known as a "hole,"<sup>14,15</sup> a Mn site, and four kinds of Al or Si sites<sup>22</sup> which will be labeled by Greek letters. Then the holes and Mn atoms just form the vertices of a packing of six RD and eight PR which forms a 1/1 cubic projection. The holes are at [000] and  $[\frac{1}{2} \frac{1}{2} \frac{1}{2}]$ , forming a perfect bcc lattice, which can be considered as two interpenetrating simple-cubic (sc) lattices; each sc edge is the long axis of an RD. The other symmetry axis of the RD are aligned with other [100] directions in such a way that the three families of RD along the three edge directions are related by threefold rotation about [111]. A view of the RD tiling within one cubic unit cell is shown in Fig. 4(a). The remaining space not filled up by the RD is filled by eight PR joining the body center and corner holes [Fig. 4(a) inset].

In the decoration of each RD [Fig. 3(a)], then, a hole occurs at each "tip" (on the long axis) while a Mn atom [Mn(1,2) in Ref. 14] sits at each of the twelve remaining vertices. The midpoint of each edge joining the tip to an Mn vertex is occupied by an Al( $\alpha$ ) = Al(4,5) atom. On each of the eight faces ad-

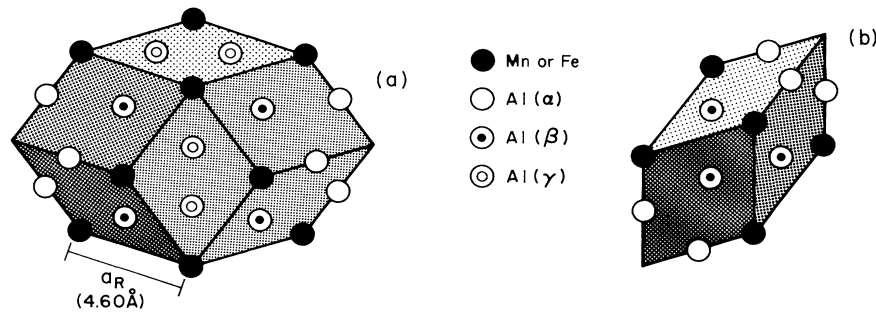


FIG. 3. (a) Rhombic dodecahedron and (b) prolate rhombohedron, showing their decoration by Al and Mn or Fe in the  $\alpha$ -(AlMnSi) or  $\alpha$ -(AlFeSi) structures. Each edge has length  $a_R$  and lies along one of the six icosahedral fivefold directions. The Al( $\beta$ ) and Al( $\delta$ ) atoms in the interior are not shown.

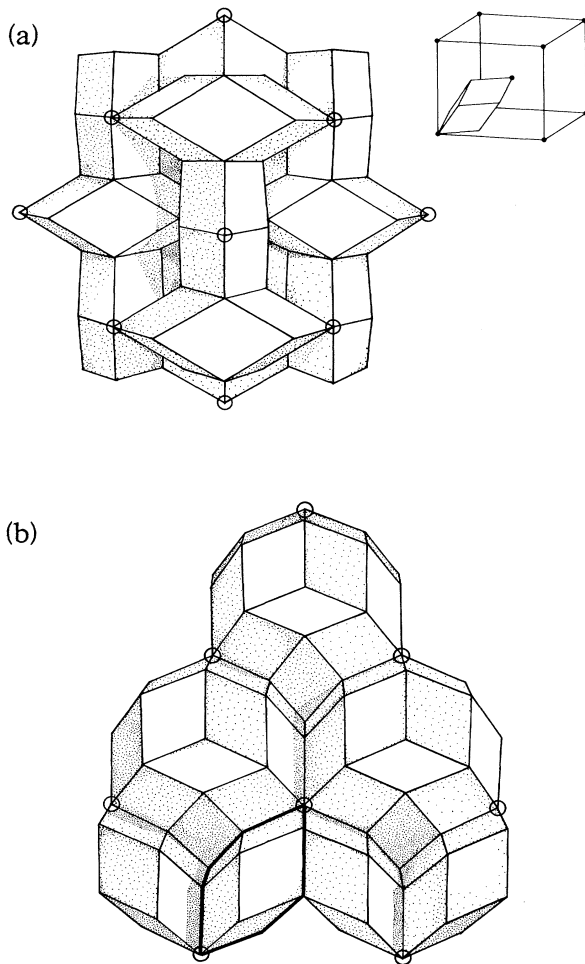


FIG. 4. Packings of rhombic dodecahedra in two crystal structures. A 54-atom Mackay icosahedron cluster (Fig. 5) is centered on each of the RD tips (circled vertices). (a) The  $\alpha$ -(AlMnSi) structure. The RD tips form a bcc lattice with the two simple-cubic sublattices connected by prolate rhombohedra (inset). (b) A layer of the  $\alpha$ -(AlFeSi) structure. One of the RD is shown outlined.

joining the tips, an Al( $\beta$ ) = Al(8,9) atom divides the diagonal from tip to (far) Mn into the ratio  $\tau^{-1}:\tau^{-2}$ . Two more Al( $\beta$ ) = Al(1,2) atoms are located in the interior of the RD on the long axis, dividing this into ratios  $\tau^{-2}:\tau^{-3}:\tau^{-2}$ . Each of the remaining four faces of the RD is decorated by two Al( $\gamma$ ) = Al(6,7) atoms dividing the long face diagonal into thirds. The RD in one of the sc sublattices contains two Al( $\delta$ ) = Al(3) atoms in their interior on the symmetry axis which is vertical in Fig. 3(a). As for the extra PR [Fig. 3(b)], they have no interior atoms; their faces are all shared with RD, which determines their decoration.

The rms deviations of the actual atomic positions from our ideal ones, averaged over all atoms of a given class, are Mn, 0.21 Å; Al( $\alpha$ ), 0.15 Å; Al( $\beta$ ), 0.15 Å; Al( $\gamma$ ), 0.68 Å. This [and similar considerations for  $\alpha$ -(AlFeSi), below] demonstrates that the rhombohedra not only have the correct size, but are essentially undistorted in shape.

In the hexagonal  $\alpha$ -(AlFeSi) structure<sup>15</sup> ( $a = 12.40$  Å,  $c = 26.23$  Å) the same RD found in  $\alpha$ -(AlMnSi) are seen to tile layers (bounded by mirror planes at  $z = \pm \frac{1}{4}$ ). Atoms of Fe [Fe(1,2,3,5) of Ref. 15] replace Mn at the vertices, and the remaining identifications are Al( $\alpha$ ) = Al(9,15), Al( $\beta$ ) = Al(6,8,12,14), Al( $\gamma$ ) = Al(10,13), Al( $\delta$ ) = Al(11). The rhombohedra are slightly smaller,  $a_R = 4.51$  Å, and now every RD contains a pair of Al( $\delta$ ) atoms. Again, the rms deviations from ideal positions are quite small: Fe, 0.24 Å; Al( $\alpha$ ), 0.21 Å; Al( $\beta$ ), 0.12 Å; Al( $\gamma$ ), 0.49 Å. In each tiled layer the holes form a triangular lattice connected by RD along the edges [Fig. 4(b)]. It is interesting to note that the RD are attached by faces different from those used in  $\alpha$ -(AlMnSi). It is not possible to extend a layer across the mirror planes by the addition of RD or PR as these solids do not have the required reflection symmetry.

We do *not* believe that our RD and PR should be viewed as independent structural entities that somehow promote icosahedral order. A better candi-

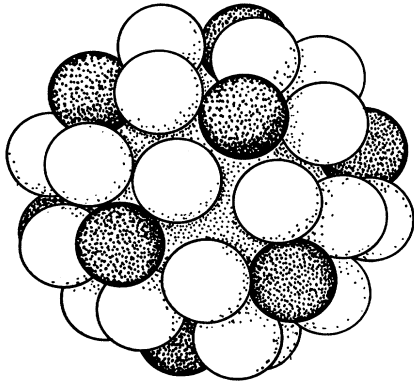


FIG. 5. The 54-atom Mackay icosahedron which appears as a structural unit in  $\alpha$ -(AlMnSi) and  $\alpha$ -(AlFeSi). The dark atoms are Mn or Fe.

date is the Mackay icosahedron<sup>23</sup> (MI), a highly symmetric  $\text{Al}_{42}(\text{Mn}/\text{Fe})_{12}$  cluster centered at each of the "holes" noted above (Fig. 5). Surrounding the vacant center site of the MI is a shell of twelve Al( $\alpha$ ) atoms, forming an essentially perfect icosahedron. A second shell consists of a larger icosahedron of twelve Mn or Fe atoms radially outward from the Al( $\alpha$ ) atoms, along with thirty Al( $\beta$ ) atoms at the edge positions of the larger icosahedron.

It is now apparent that  $\alpha$ -(AlMnSi) is simply a bcc packing of MI while  $\alpha$ -(AlFeSi) consists of MI stacked in triangular layers. Regarding (periodic or aperiodic) tilings with Penrose rhombohedra as frameworks for placing MI in space, we see that neighboring MI can be related in only two possible ways: with their centers at the far tips of (1) a RD [Fig. 3(a)] or (2) a PR [Fig. 3(b)]. In the first case Al( $\gamma$ ) [and sometimes Al( $\delta$ )] atoms are used as "glue," filling the interstices between the MI. We conjecture that  $i$ -(AlMnSi) is an alternative packing of MI and are currently exploring such structures.

We are especially grateful to Liz Hill for drawing Figs. 4 and 5 and to M. A. Marcus for many eclectic discussions.

*Note added.*—Recent experiments<sup>24–26</sup> have confirmed the close relationship between  $\alpha$ -(AlMnSi) and  $i$ -(AlMnSi). Independently, Guyot and Audier<sup>25</sup> have described the  $\alpha$ -(AlMnSi) structure in terms similar to ours. We also note that a similar analysis<sup>27</sup> of the Frank-Kasper phase<sup>28</sup>  $(\text{Al},\text{Zn})_{49}\text{Mg}_{32}$  is now relevant

as an icosahedral phase of the same composition has been discovered.<sup>29</sup>

(a)Present address: Clark Hall, Cornell University, Ithaca, N.Y. 14853.

<sup>1</sup>D. Shechtman, I. Blech, D. Gratias, and J. W. Cahn, Phys. Rev. Lett. **53**, 1951 (1984); R. D. Field and H. L. Fraser, Mater. Sci. Eng. **68**, L17 (1984).

<sup>2</sup>D. Levine and P. J. Steinhardt, Phys. Rev. Lett. **53**, 2477 (1984).

<sup>3</sup>P. A. Kalugin, A. Yu. Kitaev, and L. C. Levitov, Pis'ma Zh. Eksp. Teor. Fiz. **41**, 119 (1985) [JETP Lett. **41**, 119 (1985)].

<sup>4</sup>P. Bak, Phys. Rev. Lett. **54**, 1517 (1985).

<sup>5</sup>D. Levine *et al.*, Phys. Rev. Lett. **54**, 1520 (1985).

<sup>6</sup>N. D. Mermin and S. M. Troian, Phys. Rev. Lett. **54**, 1524 (1985).

<sup>7</sup>M. V. Jarić, Phys. Rev. Lett. **55**, 607 (1985).

<sup>8</sup>S. Sachdev and D. R. Nelson, Phys. Rev. B **32**, 4592 (1985).

<sup>9</sup>V. Elser, to be published.

<sup>10</sup>M. Duneau and A. Katz, Phys. Rev. Lett. **54**, 2688 (1985).

<sup>11</sup>V. Elser, Phys. Rev. B **32**, 4892 (1985).

<sup>12</sup>P. A. Bancel *et al.*, Phys. Rev. Lett. **54**, 2422 (1985).

<sup>13</sup>K. Robinson and P. J. Black, Philos. Mag. **44**, 1392 (1953); in particular Fig. 2.

<sup>14</sup>M. Cooper and K. Robinson, Acta Crystallogr. **20**, 614 (1966).

<sup>15</sup>R. N. Corby and P. J. Black, Acta Crystallogr., Sect. B **33**, 3468 (1977).

<sup>16</sup>P. Kramer and R. Neri, Acta Crystallogr., Sect. A **40**, 580 (1984).

<sup>17</sup>We use the axis convention of Refs. 9 and 11.

<sup>18</sup>M. Kuriyama and G. G. Long, to be published.

<sup>19</sup>C. L. Henley, J. Non-Cryst. Solids **75**, 91 (1985).

<sup>20</sup>The computer program was provided by J. M. Gibson.

<sup>21</sup>C. H. Chen and H. S. Chen, to be published.

<sup>22</sup>X-ray scattering has not distinguished Al and Si sites.

<sup>23</sup>A. L. Mackay, Acta Crystallogr. **15**, 916 (1962).

<sup>24</sup>D. C. Koskenmaki, H. S. Chen, and K. V. Rao, to be published.

<sup>25</sup>P. Guyot and M. Audier, Philos. Mag. B **52**, L15 (1985).

<sup>26</sup>M. A. Marcus, H. S. Chen, G. P. Espinosa, and C. L. Tsai, to be published.

<sup>27</sup>C. L. Henley and V. Elser, to be published.

<sup>28</sup>G. Bergman, J. L. T. Waugh, and L. Pauling, Acta Crystallogr. **10**, 254 (1957).

<sup>29</sup>P. Ramachandrarao and G. V. S. Sastry, Pramana **25**, L225 (1985).